Coulomb Excitation of Nuclei by Li^6 and Li^7 Projectiles

C. S. LITTLEJOHN AND G. C. MORRISON
Enrico Fermi Institute for Nuclear Studies, University of Chicago, Chicago, Illinois
(Received July 29, 1959)

In order to examine the characteristics of lithium-ion-induced Coulomb excitation, and to extend the cross-section ratio technique for the determination of the multipolarity of transitions, a study has been made of the γ rays emitted following electric excitation of several different target nuclei by Li^6 and Li^7 ions in the energy range 1.1 to 2.2 Mev. Measurements have been made of thick-target yields of the 110-kev ($E1$) and 198-kev ($E2$) γ rays from F^{19}, the 128-kev ($E2$) γ ray from Mn^{55}, and the 160-kev ($E2$) γ ray from Ti^{47} and compared with yields calculated from the theoretical cross sections. The yields of the γ rays studied were observed to increase with beam energy in the manner predicted by theory for electric dipole or electric quadrupole excitation. The ratios of the Li^6 and Li^7 induced yields at corresponding (equal ξ) energies for $E1$ and $E2$ transitions after correction for range effects were found to agree, within the estimated errors, with the theoretical predictions for cross-section ratios.

INTRODUCTION

EXTENSIVE investigations of the Coulomb excitation of low-lying nuclear levels have been carried out during the past few years, particularly with protons, deuterons, and helium nuclei as projectiles.[1,2] A relatively smaller amount of work has been done to date with heavier projectiles,[3–5] and in particular no results at all have been reported in the literature on the Coulomb excitation process with lithium ions. In this paper we wish to present results on the lithium-induced Coulomb excitation of levels in several light nuclei, in which the de-excitation γ rays from the states thus populated have been studied.

As has been discussed by several authors, there are a number of advantages in the use of heavy ions as projectiles in Coulomb excitation studies. These advantages will be expected to apply to the use of lithium ions. In the first place, because of the higher Coulomb barrier between the lithium projectile and the target nucleus, inelastic scattering processes compete with Coulomb excitation only at much higher incident energy than for protons and α particles. Thus there should be no appreciable contribution to the yield of Coulomb excitation from nuclear inelastic scattering. In particular, in the range of lithium bombarding energies used here, the Coulomb barrier effectively precludes any nuclear reactions.[6]

In the second place the yield of background radiation from heavy-ion bombardment is expected to be much lower than in the case of proton bombardment since both the bremsstrahlung yield[1] and the yield of characteristic x-rays are reduced for heavy ions.[7,8] Furthermore, the absence of competing nuclear reactions as discussed above should give no background of γ radiation or annihilation quanta arising from nuclear reactions produced in the target.

No appreciable self-excitation is expected for the lithium projectiles. This is apparent in the case of Li^6, which has no levels below 2.19 Mev. In the case of Li^7, the one relatively low-lying level at 0.478 Mev is reached by a magnetic dipole transition from the ground state and hence is reduced relative to the electric transitions.[1] In addition, as a result of the relatively low projectile energy used in this work, second order excitation effects are also expected to be negligible.[3] Thus in these bombardments, essentially only the Coulomb excitation of the levels of interest should occur, and the spectra of de-excitation γ rays should be relatively free from spurious effects.

For electric multipoles ($E\lambda$) the Coulomb excitation cross section may be written as[1]

$$\sigma_{E\lambda}=\left(\frac{Z_1e}{\hbar v_i}\right)^2 a^{-2\lambda+2}B(E\lambda)f_{E\lambda}(\xi), \qquad (1)$$

where

$$a=Z_1Z_2e^2/m_0v_iv_f, \qquad (2)$$

$$\eta_{i,f}=Z_1Z_2e^2/\hbar v_{i,f}, \qquad (3)$$

and

$$\xi=\eta_f-\eta_i=\frac{Z_1Z_2e^2}{\hbar}\left(\frac{1}{v_f}-\frac{1}{v_i}\right). \qquad (4)$$

In the above expressions Z_1 and Z_2 are the atomic numbers of the incident and target nuclei respectively, m_0 is the reduced mass of the incident ion, v_i and v_f are the relative velocities before and after the collision, respectively, λ is the multipole order of the transition, $B(E\lambda)$ is the reduced width for the excitation of the

[1] Alder, Bohr, Huus, Mottelson, and Winther, Revs. Modern Phys. **28**, 432 (1956), for extensive references as well as a general discussion of theory and experiment.
[2] N. P. Heydenburg and G. M. Temmer, *Annual Review of Nuclear Science* (Annual Reviews, Inc., Palo Alto, 1956), Vol. 6.
[3] Proceedings of the Conference on Reactions Between Complex Nuclei, Gatlinburg, Tennessee, May 5–7, 1958, edited by Zucker, Livingstone, and Howard [issued as Oak Ridge National Laboratory Report ORNL-2606, September, 1958 (unpublished)].
[4] J. O. Newton, University of California Radiation Laboratory Report UCRL-3797, 1957 (unpublished).
[5] Alkhayov, Andreyev, Grinberg, and Lemberg, Nuclear Phys. **2**, 65 (1956/57).
[6] E. Norbeck, Jr., and C. S. Littlejohn, Phys. Rev. **108**, 754 (1957).
[7] W. Henneberg, Z. Physik **86**, 592 (1933).
[8] D. L. Hill, Phys. Rev. **93**, 923 (1954).

level and $f_E(\xi)$ is a function of the orbit integrals involved, to first order a function of ξ alone.

The analysis of experimental results derived from a study of Coulomb excitation is first a test of the theoretical description of the excitation process and second, insofar as the description is valid, it may lead to a determination of the nuclear parameters involved in the theory. Primary results include a measurement of the energies of excited states, while further analysis leads to values of the transition probabilities and multipolarities of the transitions. The multipolarity of the transition may be determined in several ways; for example, from a study of the angular distribution of the de-excitation γ radiation or from a study of the shape of the excitation function which, for small values of ξ, is sensitive to the multipolarity of the transition. However, an alternative and in many cases preferable method is provided by a comparison of the yields for two different bombarding particles at appropriately selected energies.

It follows from Eq. (1) that if one selects bombarding energies for the two projectiles corresponding to equal values of the parameter ξ, then the ratio of the Coulomb excitation cross sections is independent of both the $B(E\lambda)$ and $f_{E\lambda}(\xi)$ factors, and is a simple function of the multipolarity of the excited transition. For convenience of reference and comparison, some corresponding Li^6 and Li^7 energies for equal values of ξ for Coulomb excitation of the 110-kev and 198-kev states in F^{17}, the 128-kev state in Mn^{55}, and the 160-kev state in Ti^{47} are listed in Table I.

In the determination of the multipolarity of the transition, the ratio method has the experimental advantage that a knowledge of the detector efficiencies is unnecessary. This is of some importance since, particularly in the case of weak, low-energy transitions, corrections for absorption of the emergent gamma radiation in the experimental equipment and target itself pose a difficult problem.

The ratio technique has been applied by several groups using variously protons, deuterons, α particles, and recently, helium-3 nuclei.[9–11] In the case of Li^6 and Li^7 bombardments, the absolute values of the ratios for transitions of different multipolarities are not so widely separated as those obtainable in bombardment by the lighter projectiles. As an example, in the 198-kev transition in F^{19}, the calculated cross-section ratio for an $E1$ transition is 1.6 times that for an $E2$ transition for proton and α excitation, whereas for Li^6 and Li^7 excitation the calculated $E1$ ratio is only 1.08 times the corresponding $E2$ ratio.

There are several advantages, however, in the employment of Li^6 and Li^7 as the projectiles in the ratio method. In the first place, thick targets may be used in the experiment since the ranges of Li^6 and Li^7 ions of equal ξ values are nearly equal and may be simply related. Thus the computed ratio of the cross section for lithium projectiles may be easily transformed to a computed ratio of thick target yields. Second, while the ratio method used with proton and alpha projectiles requires different energy ranges for selection of corresponding energies, with lithium ions the corresponding energies are reasonably close. This feature combined with the practicability of a single Li^6 and Li^7 ion source is a definite advantage experimentally. Finally, as has been discussed previously, the low background radiation expected from both Li^6 and Li^7 bombardments should greatly facilitate an accurate determination of the cross-section ratios.

The measurements reported herein were carried out primarily to examine the characteristics of Li^6- and Li^7-induced Coulomb excitation, and in particular to study the validity of the ratio technique for $E1$ and $E2$ transitions. Transitions of known multipolarity were selected in convenient target nuclides; for $E2$ transitions these included F^{19} (198 kev), Ti^{47} (160 kev) and Mn^{55} (128 kev) and for $E1$ transitions the single transition studied is that of 110 kev in F^{19}. The upper limit of 2.2 Mev on the energy of the lithium beam inhibited the study of nuclei of higher atomic number.

TABLE I. Corresponding Li^6 and Li^7 energies for equal ξ values.

E_{Li^7} (Mev)	ξ	E_{Li^6} (Mev)	E_{Li^7} (Mev)	ξ	E_{Li^6} (Mev)
F^{19} (110-kev state)			F^{19} (198-kev state)		
2.0	0.315	1.854	2.0	0.594	1.860
1.6	0.448	1.480	1.6	0.854	1.484
1.2	0.705	1.113	1.2	1.376	1.116
Mn^{55} (128-kev state)			Ti^{47} (160-kev state)		
2.0	0.831	1.886	2.0	0.964	1.877
1.6	1.179	1.507	1.6	1.372	1.501

EXPERIMENTAL ARRANGEMENT AND EQUIPMENT

Singly charged lithium ions were obtained from a 2-Mev Van de Graaff accelerator and passed through a 91.4-cm radius electrostatic analyzer which deflected them 90° before the isotopic beams were magnetically separated. The geometry was such that the range of energies incident on the target was 0.45% of the mean energy, that is, a spread of 9 kev from a 2.0-Mev beam. The lithium ions were emitted from a hot filament which had been coated with a fused mixture of SiO_2, Al_2O_3, and Li^6 enriched Li_2O, having the composition of the mineral β-eucryptite.[12] Selection of the desired projectiles was accomplished by magnetic deflection of the beam through an angle of $22\frac{1}{2}°$, after which it passed through two collimators and insulating sections before impinging on the target.

The target chamber consisted of a thin-walled brass

[9] J. H. Bjerregaard and T. Huus, Phys. Rev. **94**, 205 (1954).
[10] G. M. Temmer and N. P. Heydenburg, Phys. Rev. **96**, 426 (1954).
[11] Bromley, Kuehner, and Almquist, Phys. Rev. **115**, 586 (1959).
[12] J. P. Blewett and E. J. Jones, Phys. Rev. **50**, 465 (1936).

cylinder approximately $\frac{1}{2}$ inch in diameter and 4 inches long, which served as a Faraday cup. The target was held firmly in place against the back of the chamber by a brass expansion ring. As the emission of secondary electrons varies with the energy of the beam and differs for the Li^6 and Li^7 beams, different experimental arrangements and varying biases were tried in order to obtain an arrangement which would give reliable beam current integration independent of secondary emission. In the final arrangement the target was separated from the collimating beam stop by two insulating sections, between which was a second collimator of slightly larger diameter which could be maintained at a variable bias in order to prevent secondary electrons from the target escaping or secondary electrons emitted at the main beam defining collimator from reaching the target chamber. It was found that a bias of -180 v effectively inhibited emission of secondary electrons at all bombarding energies.

No further improvement in accuracy was made in the standard integrating circuit used, as absolute yields were not measured. All runs used in the final yield analysis were made at approximately the same beam current in order to avoid errors from nonlinearity in the current integrator circuit. To check further on the reproducibility of results, and to allow an estimate of target deterioration, control runs of 2-Mev Li^7 ions were taken between sets of runs of corresponding energies (same ξ).

In studying the Coulomb excitation of F^{19}, thick targets of NbF_5 were prepared by evaporating concentrated HF on niobium blanks. The fluoride layer thus prepared was reasonably stable under lengthy bombardments as long as the beam intensity was kept below $\frac{1}{2}$ microampere. Niobium was used as a target backing because it has no Coulomb excitation gamma radiation or characteristic x-rays in the energy region of interest (40 to 300 kev) and has a sufficiently high Coulomb barrier to inhibit nuclear reactions. In studying the Coulomb excitation of Mn^{55} and Ti^{47}, thick targets of metallic manganese and natural titanium were used.

The de-excitation gamma rays were detected at 0° to the incident beam in a conventional 2 inch by $1\frac{1}{2}$ inch NaI(Tl) scintillation spectrometer which had a resolution of 13% at 200 kev. Nearly 2π geometry was used in order to minimize any errors associated with the angular distribution of the gamma rays. The crystal face was located at about 4.5 mm from the target surface, and this distance was kept constant throughout a series of runs, since, under conditions of near geometry, small displacements of the crystal relative to the target give a sizable change in counting efficiency. Several additional runs were made with a 3 in.×3 in. NaI(Tl) crystal assembly which was similarly located. Both phototubes were magnetically shielded from the fringe field of the deflecting magnet. Standard electronic circuits were used in pulse amplifications, and the output pulses were displayed on an RCL 256-channel pulse-height analyzer.

In order to shield against room background and low-energy x-radiation coming from the accelerator, a house of 2-inch lead bricks was built around the entire counter-target assembly. Keeping the lead at a minimum distance of 6 in. from the target and surrounding the crystal with a thin copper shield effectively removed the lead fluorescent radiation which otherwise gives rise to a peak in the vicinity of 80 kev comparable to the peak arising from the 109-kev transition in F^{19}.

As mentioned in the introduction, the cross section for dipole bremsstrahlung from lithium ions is expected to be low, and higher multipole bremsstrahlung goes down as v^2/c^2, and hence is negligibly low for slowly moving lithium ions.

The dipole bremsstrahlung cross section to be expected from Li^6 and Li^7 ions incident on F^{19} as compared to that expected from He^4 ions has been calculated from the formula

$$d\sigma_{E1}=CZ_1^2Z_2^2\left(\frac{Z_1}{A_1}-\frac{Z_2}{A_2}\right)^2\frac{A_1}{E}f_{E1}(\xi)\frac{dE_x}{E_x}, \quad (5)$$

where the notation is as defined in Eq. (1), C is a numerical constant and E_x is the energy of the bremsstrahlung quantum. Of the previously used projectiles,

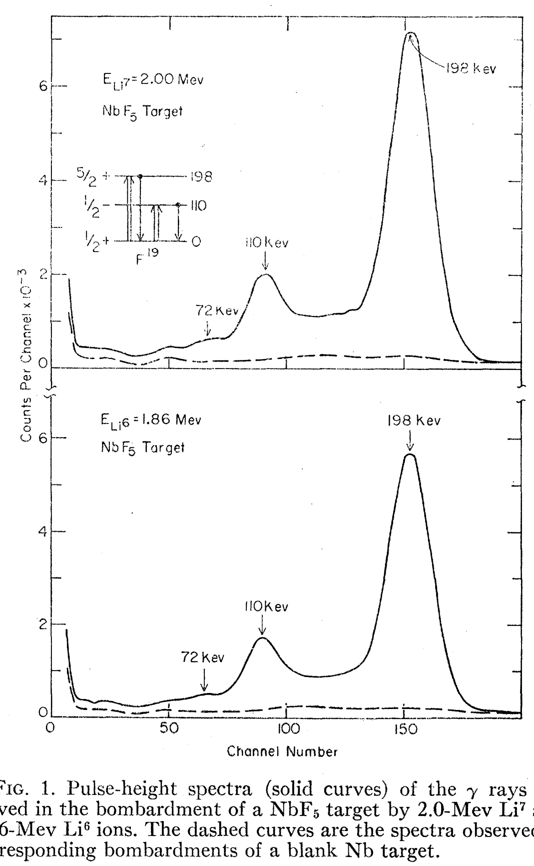

FIG. 1. Pulse-height spectra (solid curves) of the γ rays observed in the bombardment of a NbF_5 target by 2.0-Mev Li^7 and 1.86-Mev Li^6 ions. The dashed curves are the spectra observed in corresponding bombardments of a blank Nb target.

the lowest bremsstrahlung yield is that observed with α particles. At the same value of ξ, the dipole cross sections for Li^7, Li^6, and He^4 are in the ratio of 7.0:2.3:1.0. However at the same value of ξ the energy of the Li^6 or Li^7 ions is about 3/2 the energy of the He^4 ion and the cross section for Coulomb excitation by Li^6 or Li^7 is about a factor of 2 times the cross section for excitation by He^4. Thus at the same bombarding energy the bremsstrahlung is relatively reduced for incident lithium ions compared to even He^4 ions.

That the bremsstrahlung background is indeed low in the region of interest can be seen from Figs. 1–3. Background from characteristic x-rays produced by the lithium ions in the target material is also comparatively small and, for the targets used, at lower energies than the region of γ-ray energies studied.

Backscattered γ radiation constitutes a problem only in the case of the F^{19} dipole transition where the lower energy peak is superimposed on the spectral tail deriving from the higher energy γ ray. However, this uncertainty in the dipole yield is serious only at the higher energies studied and is a second-order effect in the determination of the ratio of the yields at corresponding energies.

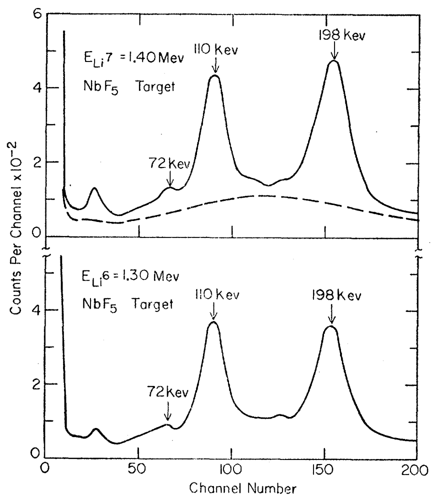

FIG. 2. Pulse-height spectra of the γ rays observed in the bombardment of a NbF_5 target by 1.4-Mev Li^7 and 1.3-Mev Li^6 ions. The dashed curve is a corresponding background spectrum.

Calibration sources of Cs^{137} (660 kev) and Am^{241} (60 kev) were used to establish the detector energy calibration. Use was also made of the shape of the observed γ-ray spectra from the Coulomb excitation of manganese as an aid in determining the spectral shapes arising from the detector and shielding in use.

RESULTS

A. Spectral Shapes

Typical pulse-height spectra of the de-excitation γ rays as observed in the 2 in.$\times 1\frac{1}{2}$ in. crystal arising from the bombardment of the different targets are shown in Figs. 1, 2, and 3. The spectra are displayed on the RCL 256-channel analyzer. Each figure shows the spectra obtained with Li^6 and Li^7 ion beams at energies corresponding to equal ξ values and for equal total integrated beam on the target. In the case of the Coulomb excitation of F^{19}, the dashed curves represent the background in the bombardment of a niobium target alone for the same integrated beam as the bombardment of the NbF^5 target. The inset to each figure shows the transitions involved where the level assignments are taken from the appropriate nuclear compilations[13,14]; the transition in Ti^{47}, which is not indicated, is between the $5/2^-$ ground state and the $7/2^-$ first excited state.

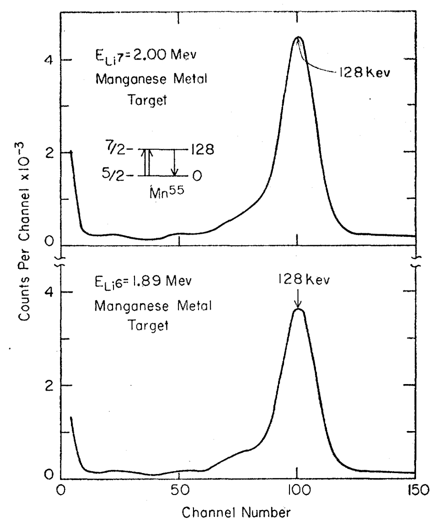

FIG. 3. Pulse-height spectra of the γ rays observed in the bombardment of a manganese metal target by 2.0-Mev Li^7 and 1.89-Mev Li^6 ions.

The principal problem encountered in obtaining yields from the observed spectra was in estimating the actual area of the photopeak of the γ rays being measured.[11,15] This was particularly acute in the case of the 110-kev gamma ray from F^{19} excitation at higher bombarding energies, as can be seen from Fig. 1. As comparison sources physically similar to the targets used and having energies close to the energies of the γ rays studied were not available, an experimental estimate of the contribution of backscattered γ rays to the observed spectra was not made. The effect of backscattering was reduced as much as possible by suitably arranging the shielding and counter. The analysis of the spectra was carried out phenomenologically in the following manner.

In the case of the γ-ray spectrum arising from the de-

[13] F. Ajzenberg and T. Lauritsen, Revs. Modern Phys. **27**, 77 (1955).
[14] P. M. Endt and C. M. Braams, Revs. Modern Phys. **29**, 683 (1957).
[15] Sherr, Li, and Christy, Phys. Rev. **96**, 1258 (1954).

excitation of F^{19}, after subtraction of the blank target background, the spectrum is essentially free from counts at energy higher than the 198-kev γ-ray peak, with only the shape of the low-energy wing of the 198-kev photopeak to be determined. The over-all shape of the photopeak was obtained by symmetrizing the low-energy wing with respect to the centroid of the peak. The area thus obtained was taken to represent the yield of the 198-kev radiation. The manganese and titanium photopeaks were treated in a generally similar manner.

The yield of the 110-kev γ radiation from F^{19} was taken as represented by the peak extending above the smooth spectrum arising from the backscattering of the 198-kev γ ray from F^{19} and the spectral tail deriving from the 198-kev γ ray. These methods for assaying peak areas were used consistently throughout the analysis of the observed spectra.

B. Excitation Functions

Using the area analysis discussed in the preceding section, thick-target excitation functions have been determined for Li^6 and Li^7 induced Coulomb excitation of the 110-kev and 198-kev levels in F^{19} and the 128-kev level in Mn^{55}. These are shown in Figs. 4, 5, and 6, where observed γ-ray yield is plotted as a function of the bombarding energy.

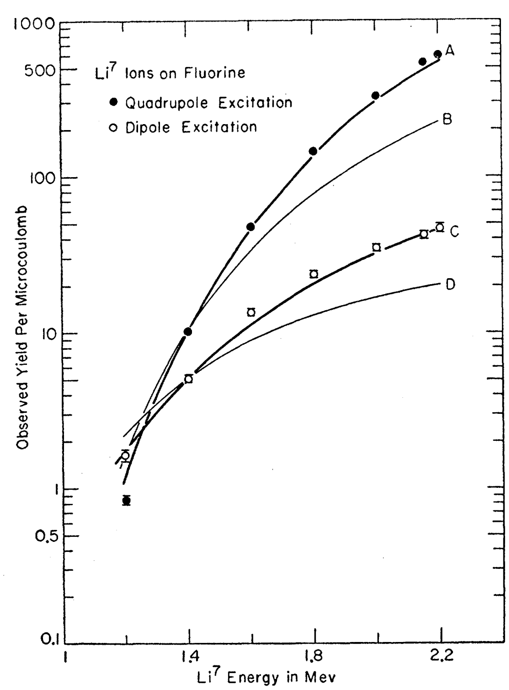

FIG. 4. Excitation functions for dipole and quadrupole Coulomb excitation of F^{19} by Li^7 projectiles. The circles are the experimentally observed thick-target yields per microcoulomb. Curves *A* and *C* are calculated thick-target yield curves normalized to the experimental points at 1.4 Mev. Curves *B* and *D* are calculated theoretical cross sections, normalized at 1.4 Mev, to compare with the shape of the thick-target yields.

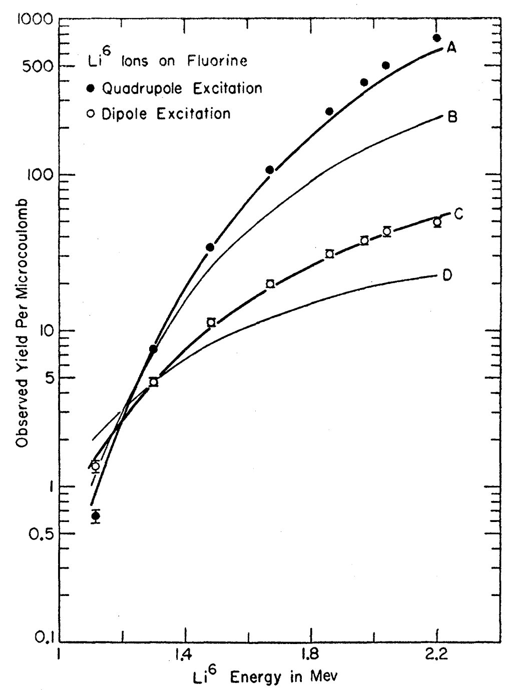

FIG. 5. Excitation functions for dipole and quadrupole Coulomb excitation of F^{19} by Li^6 projectiles. The nomenclature is the same as in Fig. 4.

No correction has been made to the experimental yields for the effect of the angular distribution of the de-excitation γ rays. For the dipole transition in F^{19} the γ-ray angular distribution is isotropic. For the quadrupole transition the angular distribution is anisotropic although the angular distribution is of course symmetric about 90°. The predicted yield at 90° is about 70% of that at zero degrees, but the yield ratios at different angles do not vary strongly with energy over the range of bombarding energies studied. In view of this and the fact that the γ rays were detected in the forward direction in nearly 2π geometry, the correction to the computed yield as a function of energy is expected to be smaller than other uncertainties arising in the experiment.

Yields in the vicinity of 2 Mev have also been measured for the excitation of the 160-kev level in Ti^{47} for both Li^6 and Li^7 bombardment. The observation of the Coulomb excitation of the 160-kev level in Ti^{47} was limited to this energy region since the small isotopic abundance of Ti^{47} in natural titanium severely reduces the yield of de-excitation γ rays relative to background radiations. The observed thick target yield in the present geometry from natural titanium was 5.20 ± 0.26 counts/μcoul for Li^6 at 1.88 Mev and 6.3 ± 0.38 counts/μcoul for Li^7 at 2 Mev.

Because of difficulties in obtaining calibrated sources of appropriate energy, the efficiency of the counting system was not determined experimentally. The experimental yields presented in Figs. 4, 5, and 6 are derived directly from the observed spectra in the NaI crystal. As the absorption of γ rays in the target and in the target chamber walls is a function of their energy, as is also the efficiency of the NaI crystal, the yields of the various de-excitation γ rays are not directly comparable.

The errors indicated on the experimental yield curves are derived from the errors due to counting statistics together with the error arising from the uncertainty in the assumed shape of the background. The combined error plotted in these curves amounts to approximately three times the standard deviation to be expected from counting statistics alone. It is thought that variations in the beam current integrator contribute only slightly to the total error. A further source of error, not indicated in these figures, arises from the uncertainty in the beam energy incident on the target, but this feature will be discussed more fully in the section concerning the ratios of spectrum yields.

DISCUSSION AND COMPARISON WITH THEORY

A. Excitation Functions

Theoretical cross sections have been calculated for the lithium-induced Coulomb excitation of the F^{19} nucleus to its 110-kev level (an electric dipole transition) and to its 198-kev level (an electric quadrupole transition) and for the electric quadrupole transitions of Mn^{55} to its 160-kev level and of Ti^{47} to its 128-kev level, over the ranges corresponding to experimental observations. The cross sections were calculated for both the Li^6 and Li^7 beams, using the numerical results of Alder *et al.*[1] and the reduced widths which they tabulate.

The theoretical cross-section curves, are shown in Figs. 4, 5, and 6, where they have been normalized to the experimental points at the energies shown. The absolute values of the theoretical cross sections over the energy range shown may be obtained from curves *B* and *D* and the absolute values of the theoretical cross sections at 2 Mev given in Table II.

Theoretical thick target yields have been calculated on the basis of these cross sections by numerical integration of the cross section over the projectile range in the target. Initial estimates were made using the theoretical treatment of thick target corrections given by Alder

TABLE II. Theoretical cross sections for Coulomb excitation by 2-Mev Li^6 and Li^7 ions.

Nucleus	Excitation energy (kev)	Multi-polarity of transi-tion	Cross section for Li^6 excitation (μb)	Cross section for Li^7 excitation (μb)
F^{19}	110	$E1$	24.3	22.2
F^{19}	198	$E2$	270	217
Ti^{47}	160	$E2$	183	130
Mn^{55}	128	$E2$	460	362

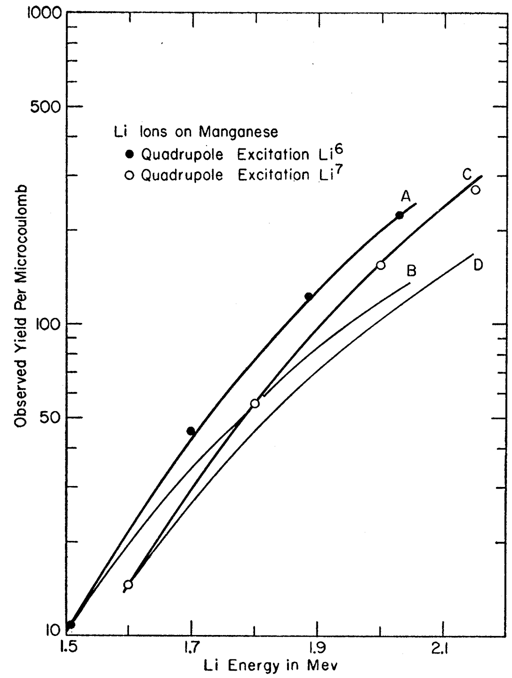

FIG. 6. Excitation functions for quadrupole Coulomb excitation of Mn^{55} by Li^6 and Li^7 projectiles. The nomenclature is the same as in Fig. 4.

et al.[1] Use was made of the relation

$$Y=\sigma(E_0)\frac{E_0N}{(dE/dx)_{E_0}}\frac{\delta E_\lambda}{E_0}, \qquad (6)$$

where Y is the fraction of the incident particles which produce the Coulomb excitation, N is the density of target atoms, $(dE/dx)_{E_0}$ is the target stopping power at the incident energy E_0 and $\delta E_\lambda/E_0$ is the ratio of the observed yield to that which would result if σ and dE/dx were independent of energy and equal to their values at E_0. Inasmuch as the values of $\delta E_\lambda/E_0$ which are tabulated by Alder *et al.* are calculated on the assumption that the projectile stopping power decreases as a function of energy as $E^{-0.55}$, which is not valid for lithium ions in the range of energies studied (the stopping power for lithium ions is still increasing with energy at these energies), a recalculation of $\delta E_\lambda/E_0$ was made taking into account the actual stopping powers for lithium ions of the various substances irradiated. These latter have not been measured, but were estimated from the best data for the stopping powers of protons in conjunction with measured values of the effective charge of the lithium ions as a function of energy.[16,17] The thick-target yields calculated on this basis are shown in Figs. 4, 5, and 6, normalized to the

[16] W. Whaling, *Encyclopedia of Physics*, edited by S. Flügge (Springer-Verlag, Berlin, 1958), Vol. 34.

[17] Teplova, Dmitriev, Nikolaev, and Fateeva, J. Exptl. Theoret. Phys. (U.S.S.R.) **32**, 974 (1957).

experimental points at the energies shown. When account is taken of the uncertainty in the energy calibration of the analyzer, the over-all agreement between the calculated and experimental thick-target yields is very good, in particular when it is observed that the experimental yield varies by factors of 100 to 1000 in the energy range studied. Furthermore the numerical factors used in the normalization of the thick-target yields to the experimental yields are identical for the Li^6 and Li^7 excitations of the 198-kev level in F^{19}; this is also the case for the 128-kev level in Mn^{55}, and the factors are very nearly the same for the excitation of the 110-kev level in F^{19}.

Estimates have been made of the γ-ray absorption expected in the target and target chamber and of the efficiency of the NaI crystal in recording the full γ-ray energy at energies corresponding to the γ rays observed. From the counting efficiencies derived in this way the absolute yield of γ rays was determined in each case. The different factors used in the normalization of the dipole and quadrupole yields in the Coulomb excitation of F^{19} can be satisfactorily related on the basis of the relative counting efficiencies for the 110- and 198-kev γ rays.

Experimental cross sections were also estimated from the absolute yield by essentially the inverse procedure to that used in calculating thick-target excitation functions, according to the formula

$$\sigma=\frac{1}{N_P N_T}\frac{dY}{dE}\frac{dE}{dx}, \tag{7}$$

where N_P is the number of projectile ions impinging on the target containing N_T atoms/cc, dY/dE is the slope of the thick-target excitation function and dE/dx is the target stopping power. The cross sections so calculated varied with energy in a manner similar to the theoretical cross sections (as is to be expected from the comparison of thick target yields with theory) and the absolute magnitude was in each case within about a factor of 2 of the theoretical values. When the uncertainties in the exact composition of the target and in the estimation of the absolute yields are considered, this order of magnitude of agreement between the magnitudes of the theoretical and experimental cross sections seems satisfactory.

TABLE III. Predicted values of cross-section ratios for corresponding energies of Li^7 and Li^6 ions.

Nucleus	Transition	$\sigma_{E\lambda}(Li^6)/\sigma_{E\lambda}(Li^7)$	R_{Li^6}/R_{Li^7} at corresponding energies	$Y_{E\lambda}(Li^6)/Y_{E\lambda}(Li^7)$
F^{19}	$E1$	0.925	92.5%	0.856
F^{19}	$E2$	0.858	92.5%	0.794
Mn^{55}	$E2$	0.832	95%	0.790
Ti^{47}	$E2$	0.832	94%	0.782

B. Cross Section Ratios

Theoretical cross-section ratios $R_{E\lambda}$ for the observed electric dipole and electric quadrupole transitions have been calculated from Eq. (1) at each bombarding energy selected (same ξ), where $R_{E\lambda}$ is taken to be $\sigma_{E\lambda}(Li^6)/\sigma_{E\lambda}(Li^7)$. The calculated ratios, which in each case are almost exactly constant over the range of energies studied, are presented in column 3 of Table III.

Before comparing the calculated cross-section ratios with experiment, however, the calculated ratios must be modified to correspond to the ratio of thick-target yields observed experimentally. In so far as the initial energies of the Li^6 and Li^7 ions incident on the target are selected at the same ξ and the thick-target yield is given by the integral of the cross section over the range

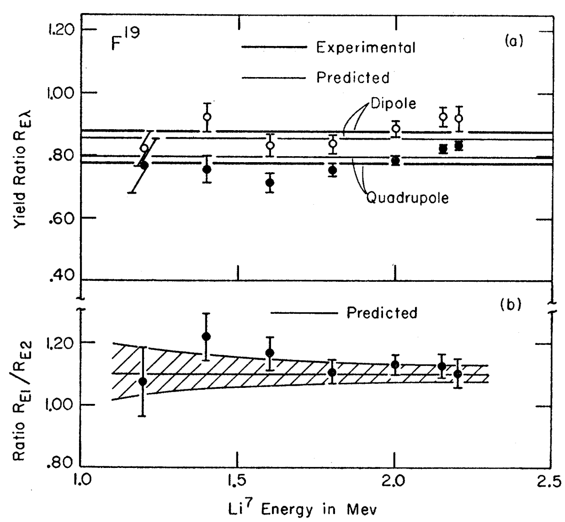

FIG. 7. (a) Thick-target yield ratio $R_{E\lambda}$ for dipole and quadrupole excitation of F^{19} as a function of Li^7 bombarding energy and the corresponding Li^6 bombarding energy. (b) R_{E1}/R_{E2} for dipole and quadrupole excitation of F^{19} as a function of Li^7 bombarding energy and the corresponding Li^6 bombarding energy.

of the projectile, the necessary correction arises from the difference in the ranges of the Li^6 and Li^7 ions in the thick target used. Because of the slightly greater range of Li^7 compared with Li^6 at the same ξ value, the incident Li^7 ions effectively are exposed to a greater number of target nuclei, giving an increased yield. On the assumption of uniform target density, the ratio of the thick-target yields is given by

$$\frac{Y_{E\lambda}(Li^6)}{Y_{E\lambda}(Li^7)}=\frac{R_{Li^6}\,\sigma_{E\lambda}(Li^6)}{R_{Li^7}\,\sigma_{E\lambda}(Li^7)}. \tag{8}$$

The ratio of the ranges of Li^7 and Li^6 at corresponding energies can be directly calculated from the expression

$$R_{Li^6}(E)=aR_{Li^7}(E/a), \quad \text{where} \quad a=M_{Li^6}/M_{Li^7}, \tag{9}$$

relating the ranges of the different ions, and the expansion

$$R(E+\Delta E)=R(E)+|(dE/dx)^{-1}|_E\Delta E, \qquad (10)$$

relating the range at energy E to that of the same ion at slightly different energy. Values of the range correction derived in this way were essentially constant at each set of corresponding energies throughout the range of energies selected. The calculated values are presented in Table III, column 4, as are the predicted values of the thick target yield ratios (column 5). The small differences in the range corrections arise from the slight variations in the ratio of the energy of Li^6 to the energy of Li^7 corresponding to the same ξ value for the different targets studied.

As a check on the validity of the range correction, the ratio of the thick-target yields of Li^7 projectiles of 2 Mev to the yield of Li^6 projectiles of 1.86 Mev (same ξ) for the NbF_5 target was calculated explicitly by numerical integration of the theoretical cross section over the path length in the target. The ratios of the yields obtained in this way for both dipole and quadrupole transitions in F^{19} were identical with those obtained from the simple correction for range differences.

Figure 7(a) shows the yield ratios determined experimentally for F^{19} compared with the predicted values of the ratios as functions of the incident Li^7 and corresponding Li^6 energies. As shown, both the electric quadrupole and electric dipole results are in reasonable agreement with the predicted values and there is no systematic deviation from a constant value of the ratio in either case.

The errors indicated in the experimental ratios are those deriving from counting statistics and background subtraction only. An additional source of error which may give rise to appreciable variation from the predicted value of the yield ratio is that arising from the uncertainty in the energy calibration of the accelerator ($\pm$9 kev at 2 Mev). In view of the rapid variation of the yield curve, this uncertainty in the exact choice of comparison energies can easily account for the larger spread in the experimental ratios than would be expected from the statistical errors alone. In this connection the good agreement obtained between the experimental and predicted values of the ratios of the Li^7 energy of 2 Mev should be noted. The experimental values in this case were derived from an average of the dipole and quadrupole yields observed in three independent runs at 1.86-Mev Li^6 and an average of the yields observed in all the check runs performed at 2-Mev Li^7.

The self-consistency of the experimental results is brought out more clearly in Fig. 7(b) where the ratio of the thick-target yield ratio for an electric dipole transition to the ratio for an electric quadrupole transition is compared with the value expected theoretically. For comparison with the experimental results the value of 1.08 computed for the ratio has to be increased slightly to 1.10. This correction arises because the experimental ratios for $E1$ and $E2$ transitions were measured at the same energy of Li^6 corresponding to the same energy of Li^7 whereas the energy of Li^6 should be slightly lower for $E1$ transitions than for $E2$ transitions. The shaded area about the predicted value of the ratio takes into account the spread in this value to be expected from the uncertainty arising in the selection of corresponding energies. It can be seen that with this additional source of error taken into account, the measured and predicted values of the ratio are in good agreement at all energies.

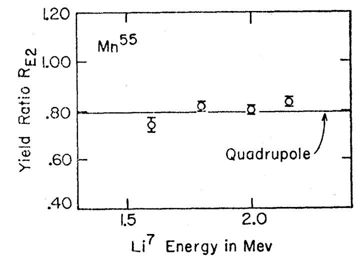

FIG. 8. Thick-target yield ratio R_{E2} for quadrupole excitation of Mn^{55} as a function of Li^7 bombarding energy and the corresponding Li^6 bombarding energy. The horizontal line is the theoretical ratio prediction for the quadrupole transition.

The yield ratios determined experimentally for Mn^{55} are shown in Fig. 8 compared with the predicted value of this ratio as a function of incident Li^7 energy. The agreement with the predicted value is again reasonable with the same qualifications as discussed above. For Ti^{47} at Li^7 energies of 2.15 and 2.0 Mev and corresponding energies of Li^6, the mean value of the ratio was $(77\pm6)\%$ to be compared with a predicted value of 78.2%.

CONCLUSION

Study of the Coulomb excitation induced by lithium ions has yielded thick-target excitation functions for electric dipole and electric quadrupole transitions which are reasonably well described by the predictions of the theory. Measurements of the yield ratios for electric dipole and electric quadrupole transitions are self-consistent and, within experimental error, in accord with the predicted cross-section ratios as corrected for range effects in thick targets. The experiments indicate that the ratio technique using Li^6 and Li^7 projectiles may provide a useful method for multipolarity determinations.

The relatively low background radiation observed with lithium ions together with the small probability for nuclear inelastic scattering are additional incentives to the use of lithium as a projectile in Coulomb excitation studies. Calculations indicate that, at an energy comparable to that available in the present study, low-energy $E2$ transitions should be excited to an appreciable extent even in the rare earth region [where higher $B(E2)$ values are found]. It should also be noted that lithium ions of 5 Mev should be capable of exciting with reasonably high yields most nuclei throughout the periodic table whose study with other projectiles has been previously reported in the literature.

ACKNOWLEDGMENTS

This work is one of the researches carried out under the sponsorship of Professor S. K. Allison. The authors are indebted to Professor Allison for valuable discussions regarding the work, and to Mr. J. Erwood and Mr. L. Herzenberg for dependable operation of the accelerator and maintenance of the electronic equipment.

PHYSICAL REVIEW VOLUME 116, NUMBER 6 DECEMBER 15, 1959

Low-Lying Energy Levels in Sc^{41}†

H. S. PLENDL,* AND F. E. STEIGERT
Yale University, New Haven, Connecticut

(Received July 9, 1959)

The reaction $Ca^{40}(d,n)Sc^{41}$ was studied at 4.15-Mev bombarding energy using nuclear emulsions as detectors. Four groups of neutrons were observed with Q values of −0.57, −2.43, −2.64, and −2.85 Mev. The observed angular distributions can be fitted with distirbution curves obtained from stripping analysis on the basis of $r_0=6.0$ fermi and $l_p=3$, 1, 1, 1, respectively. Two additional groups of questionable assignment were observed at $Q=-1.13$ and −1.41 Mev. Neutron groups from reactions on C^{12} and O^{16} were also observed and served to confirm the beam calibration as well as background and other correction methods.

THE mirror pair Ca^{41}–Sc^{41} is of interest from several points of view. To begin with, it is one of the highest mass doublets that can be investigated experimentally. Its study should, therefore, give an indication of how far one can push the ideas of charge symmetry that have been applied to lighter mass pairs so successfully. Further, the odd nucleon in each member of the pair should correspond to the beginning of the $f_{7/2}$ shell. The addition of this odd nucleon to the particularly stable 20-20 nucleon configuration of Ca^{40} might be expected to lead to a reasonably clean and uncomplicated level structure. The lowest lying states are most likely

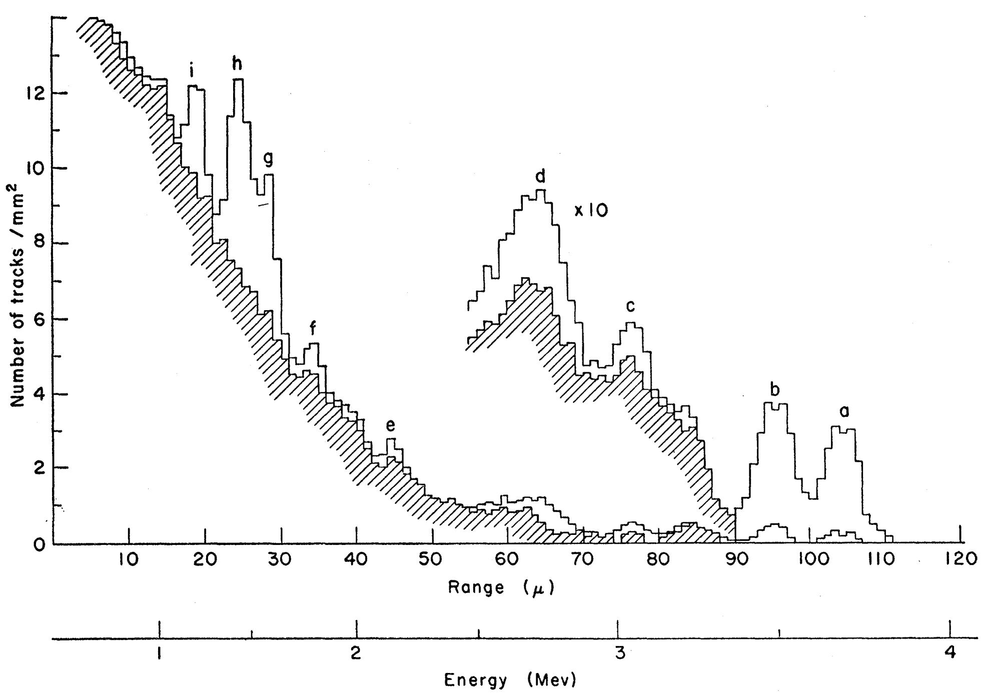

FIG. 1. Proton recoil spectrum for 35° laboratory angle. Shaded area illustrates background yield from separate background plate. Expanded portion indicates spectrum from additional scanning for tracks of 50 μ minimum length.

† This work was supported by the Office of Naval Research.
* Now at Florida State University, Tallahassee, Florida.